^{207}Pb and ^{205}Tl NMR on Perovskite Type Crystals $APbX_3$ (A = Cs, Tl, X = Br, I)

Surendra Sharma, Norbert Weiden, and Alarich Weiss
Institut für Physikalische Chemie, Physikalische Chemie III, Technische Hochschule Darmstadt, West Germany

Z. Naturforsch. **42a**, 1313–1320 (1987); received August 24, 1987

Dedicated to Prof. Dr. K. G. Weil to the Occasion of his 60th Birthday

By ^{205}Tl and ^{207}Pb NMR the chemical shift in polycrystalline samples of binary halides AX, BX_2 and ternary halides ABX_3 (A = Cs, Tl; B = Pb; X = Br, I) was studied at room temperature. The chemical shift tensors $\delta(^{205}\text{Tl})$ and $\delta(^{207}\text{Pb})$ were determined in magnitude and orientation on single crystals of the orthorhombic $TlPbI_3$. The components of the $\delta(^{205}\text{Tl})$ tensor are: $\delta_x(^{205}\text{Tl}) \parallel \boldsymbol{a} = 611$ ppm; $\delta_y(^{205}\text{Tl}) \parallel \boldsymbol{b} = 680$ ppm; $\delta_z(^{205}\text{Tl}) \parallel \boldsymbol{c} = 1329$ ppm; $\delta_{iso}(^{205}\text{Tl}) = 873.3$ ppm (with respect to 3.4 molar aqueous solution of $TlOOCCH_3$). The chemical shift tensor of ^{207}Pb in $TlPbI_3$ shows two orientations. One of them is: $\delta_x(^{207}\text{Pb}) = 3760$ ppm, inclined 30° from $\boldsymbol{b}$ towards $\boldsymbol{c}$, $\delta_y(^{207}\text{Pb}) \parallel \boldsymbol{a} = 3485$ ppm, $\delta_z(^{207}\text{Pb}) = 2639$ ppm inclined 120° from $\boldsymbol{b}$ towards $\boldsymbol{c}$. $\delta_{iso}(^{207}\text{Pb}) = 3295$ ppm (with respect to saturated aqueous solution of $Pb(NO_3)_2$). The results are discussed with respect to the crystal structure and a model to explain orientation and anisotropy of the tensors $\delta(^{205}\text{Tl})$ and $\delta(^{207}\text{Pb})$ in $TlPbI_3$ is proposed.

In the system $CsPbBr_{3-x}I_x$ $\delta(^{207}\text{Pb})$ was studied on polycrystalline samples. The chemical shift increases with increasing x and negative excess shift is observed.

Introduction

A very simple arrangement of the ions (atoms) in a solid compound ABX_3 is the cubic perovskite type structure with one formula unit in the elementary cell, with the space group O_h^1–Pm3m, and the atoms in 0, 0, 0 (A), $\frac{1}{2}$, $\frac{1}{2}$, $\frac{1}{2}$ (B) and $\frac{1}{2}$, $\frac{1}{2}$, 0; $\frac{1}{2}$, 0, $\frac{1}{2}$; 0, $\frac{1}{2}$, $\frac{1}{2}$ (X). In case of highly polarizable atoms (ions) A and X and strongly polarizing atoms (ions) B changes of temperature and/or pressure and thereby the decrease in interatomic distances leads to phase transitions. The classical example is $BaTiO_3$ in which the cubic perovskite structure changes into a polar one showing ferroelectricity and other properties connected with its strong uniaxial polarization.

Considering such physical properties, an interesting group of compounds ABX_3 are ternary halides with A = alkali metal atom, B = element of the group IV (Ge, Sn, Pb), and X = F, Cl, Br, I. The polarizabilities of A and X, respectively, increase with increasing atomic number whereas the B elements have increasing polarizing power with decreasing atomic number. Wide variations of crystal structures, phase transitions, and physical properties occur by using the wide range of chemical combinations within this group of ABX_3 compounds. Quite a large number of investigations has been devoted to the halides ABX_3 in recent years.

A well studied compound out of the group under discussion is $CsPbCl_3$. The phase transitions have been investigated by X-ray and neutron diffraction [1–7], Raman scattering [1, 8], ultrasonics [6, 9, 10], nuclear magnetic resonance, NMR [11], and nuclear quadrupole resonance, NQR [12–14]. Measurements of thermal expansion, birefringence, dielectric properties, and the specific heat have been reported [7, 10, 15–17] as well as studies of the influence of hydrostatic pressure on the phase transitions [18]. Combining EPR on $Gd^{3\oplus}$ doped $CsPbCl_3$ crystals and measurements of dielectric properties, Cohen et al. [19] observed six different phases in the temperature range $170 \leqq T/\text{K} \leqq 320$. A pyroelectric phase was observed thereby in the range $175 \leqq T/\text{K} \leqq 193$.

The transition from the cubic high temperature phase to the tetragonal phase II is – as in the system $CsPbBr_3$ [20, 21], too – of first order and of tilting type. It is connected with a soft mode condensation [5]. Following transitions to low temperature phases result in orthorhombic unit cells ($CsPbCl_3$, $CsPbBr_3$ [5, 21]), and monoclinic phases have been observed, too ($CsSnCl_3$ [22]).

Reprint requests to Prof. Dr. Al. Weiss, Institut für Physikalische Chemie III, Technische Hochschule Darmstadt, Petersenstraße 20, D-6100 Darmstadt.

0932-0784 / 87 / 1100-1313 $ 01.30/0. – Please order a reprint rather than making your own copy.

Several studies have been reported for the compounds $CsSnX_3$, with X = Cl, Br, I. Scaife et al. [23] studied these systems by X-ray diffraction and by NQR and Barrett [24] conducted Sn-Mössbauer spectroscopy on these ternary Sn(II) halides. Investigations on mixed crystals $CsSnBr_{3-x}Y_x$, Y = Cl, I, have been included in the work of these authors.

The high temperature perovskite type phase of $CsGeCl_3$ changes to a rhombohedral low temperature phase (space group R3, $Z = 1$, $T_c = 155\,^{\circ}C$), and this phase exhibits ferroelectricity with a dielectric constant comparable to that of $BaTiO_3$ [25]. Here the stronger polarizing power of $Ge^{2\oplus}$ compared to $Sn^{2\oplus}$ and $Pb^{2\oplus}$, respectively, shows up.

Some of the ternary halides ABX_3 exhibit semiconductor properties, which may be drastically influenced by halogen exchange. For example, the specific electric conductivity of the p-type semiconductor $CsSnBr_3$ drops from 10^{-1} S to 10^{-6} S by going to $CsSnCl_3$ [26]. A striking example for the effect of alkali atom exchange is $RbGeI_3$ (space group $P2_12_12_1$; $Z = 4$) and $CsGeI_3$ (P222 or Pmmm; $Z = 1$), respectively. The rubidium compound is a semiconductor whereas $CsGeI_3$ shows metallic conductivity [27].

Strong anharmonic lattice vibrations of the X-ions have been observed for $CsPbX_3$ (X = Cl, Br) [2–4], and in turn Mizusaki et al. [28] found halogen ion conductivity in these compounds; the conductivity is comparable to that of $PbCl_2$ and $PbBr_2$, respectively. ^{19}F NMR studies indicate a high mobility of the $F^{\ominus}$-ions in $CsPbF_3$ [29].

Besides the power of NMR and NQR methods in investigating phase transitions [30, 31], for ternary halides A (group I) B (group IV) X_3 (halogen) studies on compounds ABX_3 (A = Cs, Tl; X = Br, I) are scarce. Several groups investigated the phase transitions of $CsPbCl_3$ via the temperature dependence of the spin-lattice relaxation time T_1, the line width, the frequencies of the ^{35}Cl NQR lines, and of $T_1(^{133}Cs)$ [1, 11–14]. In $CsPbCl_3$ and $RbPbCl_3$ the quadrupolar splittings and the relaxation times T_1 of ^{133}Cs and ^{87}Rb, respectively, have been measured at different temperatures [32, 33]. The ^{81}Br NQR was observed in the low and the high temperature phase of $CsSnBr_3$ [23] while for $CsPbBr_3$ the $^{79,81}Br$ NQR was detected below the phase transition temperature $CsPbBr_3(I) \rightarrow CsPbBr_3(II)$, $T_c = 403$ K [34].

Measurements of the chemical shifts δ in the NMR spectra of ABX_3 halides are not reported in literature. Suitable nuclei with a nuclear spin quantum number $I = 1/2$ are available ($^{203,205}Tl$, ^{207}Pb, $^{117,119}Sn$, and ^{19}F) but experimental circumstances are prohibitive. Broad NMR-lines are expected because of scalar exchange, dipolar coupling and lattice imperfections [35]. Furthermore, for Pb and Sn, both the isotopic abundance and the gyromagnetic ratio does not favour the NMR experiment. On the other hand, the study of the chemical shift is possible for mixed crystals $A_{1-x}A'_xBX_3$, $AB_{1-y}B'_yX_3$, $ABX_{3-z}X'_z$, and so on. An experiment with mixed crystals is, however, practically excluded for quadrupolar nuclei because of severe line broadening.

In the following we report ^{207}Pb and ^{205}Tl NMR studies on AX, PbX_2, and $APbX_3$, A = Cs, Tl; X = Br, I and on mixed crystals in these ternary halides.

Experimental

Preparation, Single Crystal Growth

All compounds studied have been synthesized by melting together the stoichiometric amounts of the reagent grade constituent chemicals. TlBr, $PbBr_2$, and PbI_2, all 99%, were obtained from E. Merck, Darmstadt. CsBr (> 99%) and CsI (> 99.5%) were purchased from Fluka, Basel.

The constituents were dried and sealed in supremax glass ampoules under vaccum. They were heated to 50 K above the melting point of the respective compound ABX_3. The melt was kept at this temperature for about seven hours and shaken well at intervals to ensure homogeneity. Polycrystalline samples and samples of mixed crystal systems were made following this procedure. $TlPbI_3$ was purified ten times by zone melting (8 mm/h). The purified material was transparent and red in colour. The middle part of the zone refined regulus thus obtained was used for growing single crystals. Since $CsPbBr_3$ reacts slightly with glass [36] only four zone refining cycles were done for this material.

Large crystals of $TlPbI_3$ and $CsPbBr_3$ were grown from the zone refined material by Bridgeman technique. A temperature gradient of ~ 30 K/cm at the connecting position of the upper ($T > T_{melt}$) and the lower ($T < T_{melt}$) furnace and a lowering rate of 1 mm/h for the sample tube was found satisfactory for the growth of both materials. The crystal structure of $TlPbI_3$ has been determined by Stoeger [37] (orthorhombic, space group D_{2h}^{17}–Cmcm; $Z = 4$). The

crystals cleave easily along the plane (001) [37]. A crystal of $(10 \times 10 \times 10)\,mm^3$ in size was cut and mounted on a one circle goniometer in the magnet with the help of an optical goniometer in such a way that it could be rotated around the three orthogonal axes ***a***, ***b***, and ***c***, respectively, depending on the mounting.

^{207}Pb and ^{205}Tl NMR Measurements

The chemical shift δ of the ^{205}Tl and ^{207}Pb NMR signal has been measured in a magnetic field of 4.7 Tesla using a pulse spectrometer. The free induction decay (FID) was accumulated and transformed into the frequency domain by fast Fourier transform (FFT).

All experiments were carried out at room temperature with a spectrometer frequency of 41.890 MHz and 115.500 MHz for the ^{207}Pb and ^{205}Tl nuclei, respectively. Up to 5000 acquisitions were necessary to obtain the ^{207}Pb NMR signals with a signal to noise ratio (S/N) of about 20; fewer acquisitions are necessary to have a ^{205}Tl NMR signal of $S/N = 20$.

The chemical shift δ of the NMR signal of a particular nucleus in a certain sample is defined with respect to the NMR frequency of the nucleus in a reference compound ν_{ref} in identical external fields B_0 by

$$\delta = (\nu - \nu_{ref})/\nu_{ref}\,, \tag{1}$$

with ν = resonance frequency of the nucleus in the sample considered. A 3.4 molar aqueous solution of Tl(I)-acetate, $TlOOCCH_3$, has been used as reference sample (external standard) for ^{205}Tl and a saturated (295 K) aqueous solution of lead nitrate, $Pb(NO_3)_2$, for ^{207}Pb. Absolute NMR frequencies of 115.4655 MHz (^{205}Tl) and 41.7418 MHz (^{207}Pb) have been determined for the reference samples. An extrapolation to infinite dilution gives $\delta = 192$ ppm for ^{205}Tl and $\delta = -70$ ppm for ^{207}Pb of our references with respect to those of ideal sample signals at infinite dilution [38, 39] and own measurements.

Results

In Fig. 1 a typical NMR signal of ^{205}Tl in polycrystalline $TlPbBr_3$ is shown. The line is broad ($\sim$ 450 ppm line width), preventing a determination of the anisotropy of the chemical shift tensor in polycrystalline material. Figure 2 summarizes all chemical shift measurements done in this work on polycrystalline compounds. The values for the isotropic chemical shift δ_{iso} of ^{205}Tl and ^{207}Pb found by single crystal measurements on $TlPbI_3$ are also given. The isotropic shift is defined by

$$\delta_{iso} = \tfrac{1}{3}(\delta_x + \delta_y + \delta_z)\,. \tag{2}$$

The deviation of δ_{iso} from the δ-value of the respective polycrystalline sample causes the high anisotropy of

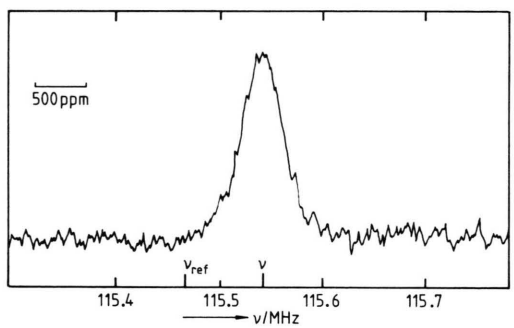

Fig. 1. NMR signal of ^{205}Tl in polycrystalline $TlPbBr_3$. The chemical shift against $\nu_{ref}(^{205}Tl) = 115.4655$ MHz is 645 ppm; the line-width is about 450 ppm. $T = 295$ K.

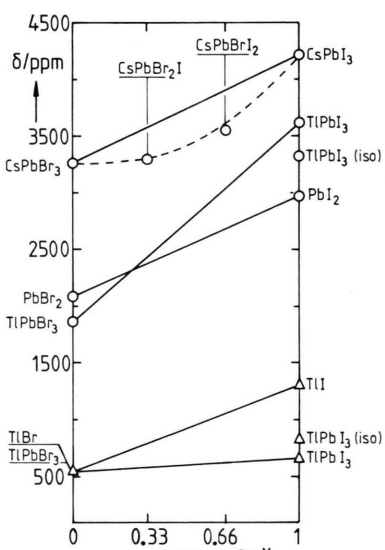

Fig. 2. Chemical shift of ^{205}Tl-NMR (△) and ^{207}Pb-NMR (○) in polycrystalline samples vs. mole fraction of right hand compound. The values for the isotropic chemical shifts δ_{iso} in $TlPbI_3$ calculated from single crystal measurements are also shown. External standards were: 3.4 molar aqueous solution of $TlOOCCH_3$, $\nu_{ref}(^{205}Tl) = 115.4655$ MHz and saturated solution of $Pb(NO_3)_2$, $\nu_{ref}(^{207}Pb) = 41.7418$ MHz. $T = 295$ K.

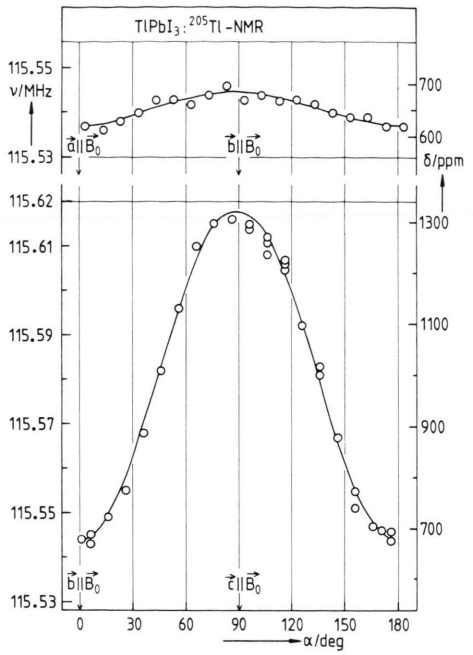

Fig. 3. Angular dependence of the thallium chemical shift $\delta(^{205}\mathrm{Tl})$ in $TlPbI_3$. *Upper part*: Rotation around ***c***-axis. *Lower part*: Rotation around ***a***-axis. $T = 295$ K.

the chemical shift tensor. Due to the line width the anisotropy could not be measured on polycrystalline samples at room temperature, and the center of the line is not identical with δ_{iso}.

The line width of the NMR signals in single crystals is 20–30% lower than that in polycrystalline samples. The angular dependence of the thallium chemical shift, $\delta(^{205}\mathrm{Tl})$, in single crystals of $TlPbI_3$ was measured using the crystal axes ***a***, ***b***, and ***c***, respectively, as rotation axes $\perp B_0$.

The results are shown in Figs. 3 and 4. It is seen that the rotation around ***a*** exhibits strong angular dependence of $\delta(^{205}\mathrm{Tl})$ and a high anisotropy of the chemical shift tensor is expected. The rotation around ***b***, the results of which are shown in Fig. 4, supports this conclusion.

The variation of the ^{207}Pb NMR chemical shift in $TlPbI_3$ with the rotation angle α is shown for the rotation around the axes ***b*** and ***c*** in Figure 5. The dependence $\delta(^{207}\mathrm{Pb}) = f(\alpha)$ with $\boldsymbol{c} \perp B_0$ is very small while the rotation around the axis ***a*** (Fig. 6) clearly points out that (a) there are two tensors for the lead NMR shift, with the tensor axes inclined 120°/60° to each other and (b) the anisotropy of the chemical shift is large for ^{207}Pb, too.

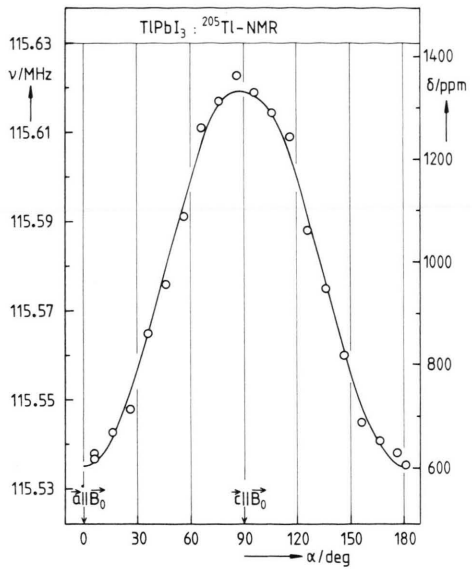

Fig. 4. Angular dependence of the thallium chemical shift $\delta(^{205}\mathrm{Tl})$ in $TlPbI_3$. Rotation around ***b***-axis. $T = 295$ K.

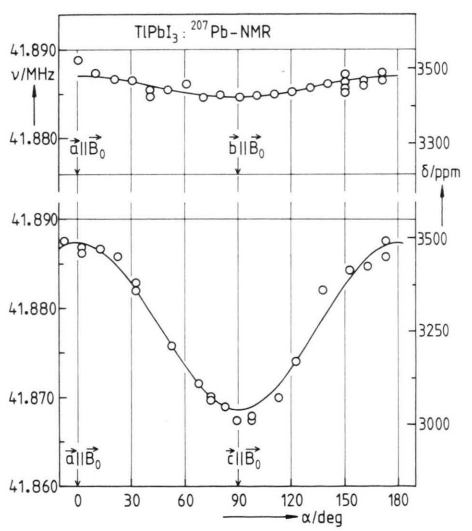

Fig. 5. Angular dependence of the lead chemical shift $\delta(^{207}\mathrm{Pb})$ in $TlPbI_3$. *Upper part*: Rotation around ***c***-axis. *Lower part*: Rotation around ***b***-axis. $T = 295$ K.

Discussion

In Table 1 we have summarized the information about the crystal structures of ternary halides ABX_3 studied here. $CsPbBr_3$ and $CsPbI_3$ are isomorphous at room temperature.

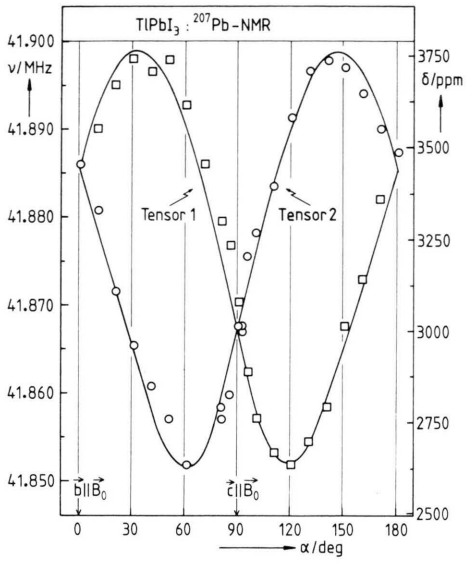

Fig. 6. Angular dependence of the lead chemical shift $\delta(^{207}Pb)$ in $TlPbI_3$. Rotation around ***a***-axis. $T = 295$ K.

Table 1. Crystal structures of ternary halides $APbX_3$ with A = Cs, Tl and X = Br, I.

Compound	Temperature range/K	Space group	Z	Reference
$CsPbBr_3$	403 and up	O_h^1 – Pm3m	1	[21]
	361–403	D_{4h}^5 – P_4/mbm	2	
	295–361	D_{2h}^{16} – Pnma	4	
$CsPbI_3$	583–749	C_{2h}^2 – $P2_1/m$	1	[44]
	295–583	D_{2h}^{16} – Pnma	4	
$TlPbI_3$	295–619	D_{2h}^{17} – Cmcm	4	[37]
$TlPbBr_3$		not known		

The chemical shift measurements on polycrystalline samples TlX, PbX_2, and ABX_3 (A = Cs, Tl; X = Br, I) show for the ^{205}Tl as well as for ^{207}Pb an increase of the shift when bromine is replaced by iodine (see Figure 2). This is the general tendency for the combinations $TlBr \rightarrow TlI$, $PbBr_2 \rightarrow PbI_2$, $TlPbBr_3 \rightarrow TlPbI_3$, and $CsPbBr_3 \rightarrow CsPbI_3$. The change of $\delta(^{207}Pb)$ is stronger than that for $\delta(^{205}Tl)$ whereas in the case of the pair $TlPbBr_3 \rightarrow TlPbI_3$ it is quite small. The data extracted from measurements on polycrystalline samples are listed in Table 2.

Hafner and Nachtrieb [38, 40] have made an extensive study of $\delta(Tl)$ for the halides of Tl(I); TlF, TlCl, TlBr, and TlI. It should be noted that the value for $\delta(^{205}Tl)$ in TlBr agrees well with that of Hafner and Nachtrieb [38] if $\delta(^{205}Tl)$ is calculated with respect to

Table 2. Resonance frequencies ν and chemical shifts $\delta(^{205}Tl)$ and $\delta(^{207}Pb)$ in polycrystalline samples of TlX, PbX_2 and $APbX_3$ with A = Cs, Tl and X = Br, I at 295 K. δ is given with respect to the external standards: 3.4 molar aqueous solution of $TlOOCCH_3$ and saturated aqueous solution of $Pb(NO_3)_2$. The values of δ with respect to infinite dilution of the standard can be found by adding 192 ppm to $\delta(^{205}Tl)$ and subtracting 70 ppm from $\delta(^{207}Pb)$.

Compound	Nucleus	ν/MHz	δ/ppm
$TlPbI_3$	^{205}Tl	115.544	680
$TlPbBr_3$	^{205}Tl	115.540	645
TlI	^{205}Tl	115.626	1390
TlBr	^{205}Tl	115.540	645
$TlPbI_3$	^{207}Pb	41.893	3622
$CsPbI_3$	^{207}Pb	41.918	4221
$TlPbBr_3$	^{207}Pb	41.820	1873
$CsPbBr_3$	^{207}Pb	41.878	3263
$CsPbBr_2I$	^{207}Pb	41.879	3287
$CsPbBrI_2$	^{207}Pb	41.890	3550
$PbBr_2$	^{207}Pb	41.829	2089
PbI_2	^{207}Pb	41.866	2975

a common standard: Aqueous solution of $Tl^{\oplus}$ ions at infinite dilution. In case of TlI there is no agreement between the data of Hafner and Nachtrieb [38], Hinton and Metz [35], and ours. The value given by Hinton and Metz measured at elevated temperatures can be taken for comparison, too, since $\delta(^{205}Tl)$ is almost independent of temperature in the cubic phase of TlI [38]. The shifts calculated with respect to a reference sample, at infinite dilution and at room temperature, are: $\delta(^{205}Tl)$ in TlBr: 815 ppm [38], 837 ppm (this work). $\delta(^{205}Tl)$ in TlI: 1770 ppm [38]; 1180 ppm (at 401 K) [35]; 1582 ppm (this work). For solid solutions $TlCl_xBr_{1-x}$ Hafner [41] found an almost linear dependence $\delta(Tl) = f(x)$. The increase of $\delta(Tl)$ by the exchange $Br \rightarrow I$ was discussed by these authors in the framework of Ramsey's theory of chemical shift [42] and a simplified Heitler-London model used by Yosida and Moriya [43]. According to them an increase of covalency by the exchange $Br \rightarrow I$ leads to an increase in $\delta(Tl)$. For the mixed crystal system $(CsPbBr_3)_{1-x}$ $(CsPbI_3)_x$ the present results show clearly that the exchange $Br \rightarrow I$ raises $\delta(^{207}Pb)$ in accordance with the observation for $PbBr_2 \rightarrow PbI_2$, for which no chemical shift data could be found in the literature. However, in contrast to the system $TlCl_xBr_{1-x}$ we do not find a linear dependence $\delta(^{207}Pb) = f(x)$ but a negative excess chemical shift which cannot be explained at present. The small increase in $\delta(^{205}Tl)$ within the system $TlPbBr_3 \rightarrow TlPbI_3$ is in contrast to

the strong one for the pair TlBr → TlI. This should be compared with the $\delta(^{207}Pb)$ in the systems $TlPbBr_3 \rightarrow TlPbI_3$ and $PbBr_2 \rightarrow PbI_2$, respectively. In both cases the increase of the shift is fairly strong. We may argue that an exchange Br → I has a strong influence on the atoms in the first coordination shell of the X-atoms but not so much in the second one. From the large change of $\delta(^{207}Pb)$ by going from $TlPbBr_3$ to $CsPbBr_3$, it is seen that a possible change of crystal structure has to be taken into account.

$CsPbBr_3$ crystallizes orthorhombic while $TlPbBr_3$ is not isomorphous as preliminary investigations have shown (see Table 1).

A further discussion concerning the influence of the exchange A → A′, B → B′, X → X′on the chemical shift of NMR in ternary halides is not meaningful at present, if the data are based on measurements with polycrystalline samples. Broad lines (see Fig. 1) prohibit the determination of the anisotropy of the chemical shift tensor, and even in the case of recognizable anisotropy the direction of the principal axes of the chemical shift tensor are not obtained. A detailed discussion of correlations between chemical shift, coordination spheres, and interatomic distances is thus not possible.

The Chemical Shift Tensors $\delta(^{205}Tl)$ and $\delta(^{207}Pb)$ in $TlPbI_3$

In Figs. 3–6 the results of the single crystal measurements, $\delta(^{205}Tl)$ and $\delta(^{207}Pb)$ in $TlPbI_3$ are shown. In Table 3 the principal axes of the chemical shift tensors in magnitude and orientation are listed. Figure 7 shows the projection of the unit cell along the axis [100]. In the space group D_{2h}^{17}–Cmcm the Tl-atoms are located at the point position 4c with symmetry mm. Only one pattern $\delta(Tl) = f(\alpha)$ is therefore expected, independent of the rotation axis (***a***, ***b***, or ***c***). The principal axes of the $\delta(Tl)$ tensor must be parallel to the crystal axes by symmetry conditions, too. The values for δ_x, δ_y, and δ_z are given in Table 3. They have been calculated according to the definition

$$|\delta_z - \delta_{iso}| \geqq |\delta_x - \delta_{iso}| \geqq |\delta_y - \delta_{iso}| . \qquad (3)$$

The $\delta(Tl)$-tensor is almost rotational symmetric, $\delta_y - \delta_x = 69$ ppm, while the tensor is strongly stretched in the z-direction, $\delta_z - \delta_x = 718$ ppm.

In Fig. 8 the orientation of the principal axes of the $\delta(^{205}Tl)$ tensor with respect to the first coordination sphere of Tl in $TlPbI_3$ are drawn. (Figure 8 should be compared with Figure 7.) One recognizes that the two axes with the nearly equal and small values of $\delta(^{205}Tl)$, $\delta_x(^{205}Tl)$, and $\delta_y(^{205}Tl)$ are located in a plane formed by the Tl atom and two iodine atoms $I^{(2)}$. $\delta_x(^{205}Tl)$ is parallel to the line $I^{(2)}$–$I^{(2)}$ and $\delta_y(^{205}Tl)$ bisects the angle $\sphericalangle(I^{(2)}-Tl-I^{(2)})$. In Table 4 the next nearest neighbour interatomic distances are listed. The distances $Tl-I^{(2)}$ are 346.7 pm which are the shortest Tl–I distances in $TlPbI_3$. The chemical shift of the ^{205}Tl NMR to the lowest frequencies (at B_0 = constant) is therefore strongly correlated to the shortest distance Tl–I which, most probably, involves the strongest interaction between Tl and I. A similar relation was obtained between the chemical shift of

Table 3. Principal axes of the chemical shift tensor of ^{205}Tl and ^{207}Pb in $TlPbI_3$ at 295 K. External standards: 3.4 molar aqueous solution of $TlOOCCH_3$ and saturated aqueous solution of $Pb(NO_3)_2$.

Tensor axis	δ/ppm	Orientation
$\delta_x(Tl)$	611	$\delta_x(Tl) \parallel \boldsymbol{a}$
$\delta_y(Tl)$	680	$\delta_y(Tl) \parallel \boldsymbol{b}$
$\delta_z(Tl)$	1329	$\delta_z(Tl) \parallel \boldsymbol{c}$
$\delta_{iso}(Tl)$	873.3	
Tensor 1		
$\delta_x(Pb)$	3760	at 30° from ***b*** towards ***c***
$\delta_y(Pb)$	3485	$\delta_y(Pb) \parallel \boldsymbol{a}$
$\delta_z(Pb)$	2639	at 120° from ***b*** towards ***c***
$\delta_{iso}(Pb)$	3295	
Tensor 2		
$\delta_x(Pb)$	3760	at 150° from ***b*** towards ***c***
$\delta_y(Pb)$	3485	$\delta_y(Pb) \parallel \boldsymbol{a}$
$\delta_z(Pb)$	2639	at 60° from ***b*** towards ***c***
$\delta_{iso}(Pb)$	3295	

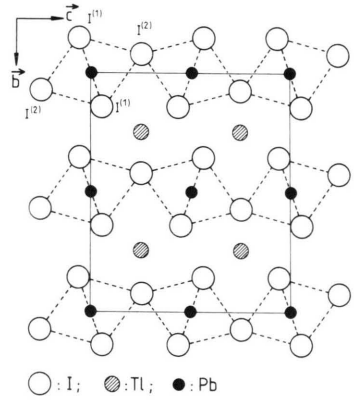

Fig. 7. Projection of the crystal structure of $TlPbI_3$ (space group D_{2h}^{17}–Cmcm, $Z = 4$ [37]) along [100].

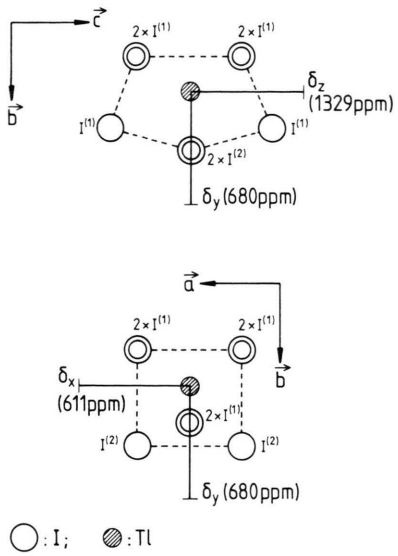

Fig. 8. Projection of the coordination polyhedron of Tl and the directions of the principal axes of the chemical shift tensor. *Upper part*: Projection along [100]. The Tl-atom and the two $I^{(1)}$-atoms drawn with single circles lie in the paper plane. The double circles for the other $I^{(1)}$- and the $I^{(2)}$-atoms indicate, that there are two atoms in each case, one above and one below the paper plane, which forms a mirror plane for the polyhedron. *Lower part*: Projection along [001]. The Tl-atom and the two $I^{(2)}$-atoms are in the paper plane, which forms a mirror plane for the polyhedron, too. The meaning of the double circles is the same as above.

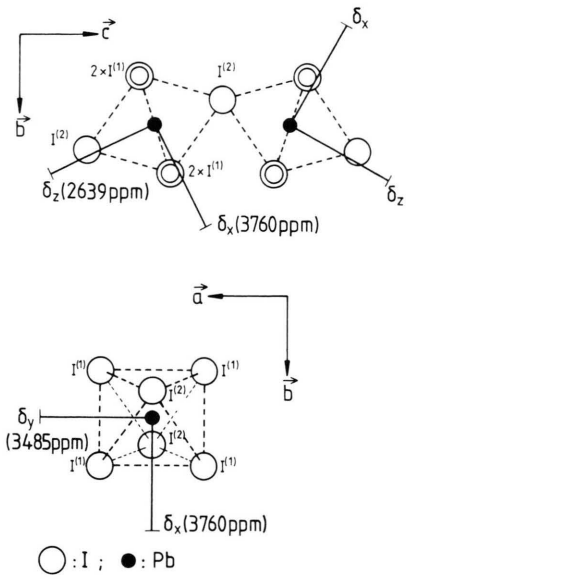

Fig. 9. Projection of the PbI_6 octahedron and the directions of the principal axes of the ^{207}Pb chemical shift tensor. *Upper part*: Projection along [100]. The Pb- and the two $I^{(2)}$-atoms lie in the paper plane, which forms a mirror plane for the octahedron. The meaning of the double circles is the same as in Figure 8. *Lower part*: Projection along [001].

Table 4. Metal-halogen distances in $TlPbI_3$ after [37].

Atom–Atom	Distance/nm	Number of distances in the coordination polyhedron
$Tl-I^{(1)}$	361.4	4
$Tl-I^{(1)}$	397.1	2
$Tl-I^{(2)}$	346.7	2
$Pb-I^{(1)}$	322.0	4
$Pb-I^{(2)}$	318.1	2

^{29}Si NMR and the Si–O distances in a single crystal of Mg_2SiO_4 [45].

Since in that case the frequency of the reference sample (Tetramethylsilane) lies above that of the solid, the highest value of $|\delta(^{29}Si)|$ belongs to the lowest frequency, in contrast to that of $\delta(^{205}Tl)$ and $\delta(^{207}Pb)$ in $TlPbI_3$.

In the framework of a superposition model a $\delta(^{205}Tl)$ tensor with rotational symmetry around an axis perpendicular to the plane defined by $I^{(2)}$, Tl, and $I^{(2)}$ would result for an angle $\sphericalangle(I^{(2)}-Tl-I^{(2)}) = 90°$. Consideration of the influence of further neighbouring atoms can alter the picture. The slight deviation of the angle $\sphericalangle(I^{(2)}-Tl-I^{(2)})$ from 90° (in $TlPbI_3$ this angle is 83.67°) may be responsible for the deviation of the $\delta(^{205}Tl)$ tensor from axial symmetry.

The Pb-atoms occupy the point position 4a with symmetry 2/m. Therefore only one of the principal axes of the $\delta(^{207}Pb)$-tensor coincides with one of the crystal axes (the axis ***a*** in $TlPbI_3$). Consequently the two other principal axes are located in the *b*, *c*-plane. For the rotation of a single crystal around [100] one therefore expects two rotation patterns $\delta(^{207}Pb) = f(\alpha)$, where α is the rotation angle. Figure 6 shows the angular dependence of $\delta(^{207}Pb)$ for rotation around [100]. It is seen therefrom that the principal axes of $\delta(^{207}Pb)$ in the plane (*b*, *c*) belong to two symmetry correlated tensors and, in consequence, to two lead atoms located at symmetry correlated points of the point position 4a. The axes form angles of 30° and 120° (tensor 1) and 150° and 60° (tensor 2), respectively, with ***b***.

From Figs. 5 and 6 it is obvious that the $\delta(^{207}Pb)$-tensor is highly anisotropic and possesses almost axial symmetry around ***c***. An answer to the question which of the two symmetry correlated tensors belongs to which of the two symmetry correlated

PbI_6-octahedra (see Fig. 7) may be found by two arguments:

1. From the crystal structure it can be concluded that the PbI_6 octahedra have a pseudofourfold axis along the direction $I^{(2)}-Pb-I^{(2)}$ (see Figure 9). The four $Pb-I^{(1)}$ bond length are equal (see Table 4). Therefore, in the first approximation, the $\delta(^{207}Pb)$-tensor should be axially symmetric around this axis. This leads to the conclusion that the two tensor axes of almost equal magnitude ($\delta_x(^{207}Pb)$ and $\delta_y(^{207}Pb)$, see Table 3) should be perpendicular to the $I^{(2)}-Pb-I^{(2)}$ direction and that the unique axis $\delta_z(^{207}Pb)$ should be parallel to it.

2. The principal axis with the lowest frequency (smallest chemical shift value) $\delta_z(^{207}Pb)$ should be correlated to the shortest Pb–I distances, in analogy to the results for $\delta(^{205}Tl)$. This leads to $\delta_z(^{207}Pb) \parallel$ direction $Pb-I^{(2)}$.

Both arguments lead to the same result. In Fig. 9 the orientation of the two symmetry correlated $\delta(Pb)$-tensors with respect to the two symmetry related PbI_6 octahedra is depicted. One notes that the idealized assumption $\delta_z(^{207}Pb) \parallel Pb-I^{(2)}$ is almost realized. The angle $\sphericalangle(\delta_z(^{207}Pb), Pb-I^{(2)})$ amounts to 8.7°. The alternative assignment leads to no correlation between structure and tensor orientation and is rejected for the above reasons.

Acknowledgement

We are grateful to the Deutsche Forschungsgemeinschaft for support of this work.

[1] M. Hidaka, Y. Okamoto, and Y. Zikumaru, Phys. Status Solidi A **79,** 263 (1983).
[2] J. Hutton, R. J. Nelmes, G. M. Meyer, and V. R. Eiriksson, J. Phys. **C12,** 5393 (1979).
[3] M. Sakata, T. Nishiwaki, and J. Harada, J. Phys. Soc. Japan **47,** 232 (1979).
[4] M. Sakata, J. Harada, M. J. Cooper, and K. D. Rouse, Acta Cryst. **A36,** 7 (1980).
[5] Y. Fujii, S. Hoshino, Y. Yamada, and G. Shirane, Phys. Rev. **B9,** 4549 (1974).
[6] T. Sakudo, H. Nuoki, Y. Fujii, J. Kobayashi, and Y. Yamada, Phys. Lett. **28A,** 542 (1969).
[7] Ch. Kn. Møller, Mat. Fys. Medd. Dan. Vid. Selsk. **32,** no. 2 (1959).
[8] S. Hirotsu, J. Phys. Soc. Japan **31,** 552 (1971).
[9] K. S. Aleksandrov, A. I. Krupnyi, V. I. Zinenko, and B. V. Beznosikov, Sov. Phys. Cryst. **17,** 515 (1972).
[10] S. Hirotsu and T. Suzuki, J. Phys. Soc. Japan **44,** 1604 (1978).
[11] R. L. Armstrong, J. A. J. Lourens, and J. D. Stroud, Phys. Rev. **B13,** 5099 (1976).
[12] R. L. Armstrong, J. Magn. Reson. **20,** 214 (1975).
[13] H. M. van Driel and R. L. Armstrong, Phys. Rev. **B12,** 839 (1975).
[14] N. Tovborg-Jensen, J. Chem. Phys. **50,** 559 (1969).
[15] S. Hirotsu and S. Sawada, Phys. Lett. **28A,** 762 (1969).
[16] S. Stokka, K. Fossheim, T. Johansen, and J. Fedder, J. Phys. C: Solid State Phys. **15,** 3053 (1982).
[17] S. V. Mel'nikova, I. N. Flerov, and A. T. Anistratov, Sov. Phys. Solid State **23,** 2074 (1981).
[18] K. Gesi, K. Ozawa, and S. Hirotsu, J. Phys. Soc. Japan **38,** 463 (1975).
[19] M. I. Cohen, K. F. Young, Te-Tse Chang, and W. S. Brower, Jr., J. Appl. Phys. **42,** 5267 (1971).
[20] S. Hirotsu, T. Suzuki, and S. Sawada, J. Phys. Soc. Japan **43,** 575 (1977).
[21] S. Hirotsu, J. Harada, M. Iizumi, and K. Gesi, J. Phys. Soc. Japan **37,** 1393 (1974).
[22] F. R. Poulsen and S. E. Rasmussen, Acta Chem. Scand. **24,** 150 (1970).
[23] D. E. Scaife, P. F. Weller, and W. G. Fisher, J. Solid State Chem. **9,** 308 (1974).
[24] J. Barrett, S. R. A. Bird, J. D. Donaldson, and J. Silver, J. Chem. Soc. (A) **1971,** 3105.
[25] A. N. Christensen and S. E. Rasmussen, Acta Chem. Scand. **19,** 421 (1965).
[26] S. J. Clark, C. D. Flint, and J. D. Donaldson, J. Phys. Chem. Solids **42,** 133 (1981).
[27] L. Guen, P. Palvadeau, M. Spiesser, and M. Tournoux, Rev. Chim. Min. **19,** 1 (1982).
[28] J. Mizusaki, K. Arai, and K. Fueki, Sol. State Ionics **11,** 203 (1983).
[29] V. M. Bouznik, Yu. N. Moskvick, and V. N. Voronov, Chem. Phys. Lett. **37,** 464 (1976).
[30] T. P. Das and E. L. Hahn, Nuclear Quadrupole Resonance Spectroscopy, Academic Press, New York 1958.
[31] M. H. Cohen and F. Reif, Sol. State Phys. **5,** 321 (1957).
[32] R. Kind, S. Plesko, and J. Roos, Ferroelectrics **13,** 433 (1976).
[33] S. Plesko, R. Kind, and J. Roos, J. Phys. Soc. Japan **45,** 553 (1978).
[34] A. F. Volkov, Yu. N. Venevtsev, and G. K. Semin, Phys. Status Solidi **35,** K167 (1969).
[35] J. F. Hinton and K. R. Metz, J. Magn. Reson. **53,** 131 (1983).
[36] F. W. Ainger, C. C. Clark, A. Marsh, and P. Waterworth, Proc. Int. Meet. Ferroelectricity, Prag, CSSR, **1,** 295 (1966).
[37] W. Stoeger, Z. Naturforsch. **32b,** 975 (1977).
[38] S. Hafner and N. H. Nachtrieb, J. Chem. Phys. **40,** 2891 (1964).
[39] O. Lutz and G. Stricker, Phys. Letters **35A,** 397 (1971).
[40] S. Hafner and N. H. Nachtrieb, J. Chem. Phys. **42,** 631 (1965).
[41] S. Hafner, J. Phys. Chem. Solids **27,** 1881 (1966).
[42] N. F. Ramsey, Phys. Rev. **78,** 699 (1950).
[43] K. Yosida and T. Moriya, J. Phys. Soc. Japan **11,** 33 (1956).
[44] Ch. Kn. Møller, Mat. Fys. Medd. Dan. Vid. Selsk. **32,** no. 1 (1959).
[45] N. Weiden and H. Rager, Z. Naturforsch. **40a,** 126 (1985).